Revised

Using a Snow Drift Model to simulate Aeolian Drift and Snowfall on the Summit of Mauna Kea, Hawaii

By

Leigh Anne Eaton and Steven Businger

University of Hawaii at Manoa

submitted to a special issue volume of the Arctic, Antarctic, and Alpine Research

June 2014

Abstract

The goal of this research is to help develop a better understanding of the micro-meteorology of the Mauna Kea summit area and its relationship to the distribution and population health of the Wēkiu Bug (*Nysius Wekiuicola)*. SnowModel, a spatially distributed snow-evolution model, is used to construct snowfall and bug-fall accumulation maps across the summit. Eight weather stations associated with astronomical observatories on the summit ridges and four Davis weather stations located in various cinder cones (puʻu in Hawaiian), provide the meteorological observations needed as input to run SnowModel. Snow-depth observations taken after a passing cold front in January 2011 are used to help validate the model accumulation predictions prior to the climatological study. Observations from the eight weather stations over a three-year period (2008, 2009, and 2010) are used as input for the modeled summit accumulations of snowfall and bug fall, presented in this study. For the snowfall maps, only weather data from days during which snow fell are included. For the bug-fall estimates, all days for which we have weather data are included in the model output. Since there are no comprehensive data available on the distribution of bug fall, the bug-fall maps only provide a climatological pattern, without reference to the magnitude of the bug fall.

The greatest modeled snow accumulations are found on Puʻu Wēkiu and Puʻu Haukea. Similar results are found in the climatological bug-fall accumulation pattern. Prevailing wind direction is most critical for the distribution of snowfall and bug fall with maximum accumulations occurring on lee side of ridges and crests. Favorable Wēkiu Bug trapping sites in which bugs were found historically, are spatially well collocated

with snowfall and bug fall accumulations, suggesting that the results of this study will be of interest to entomologists in locating wēkiu bug populations.

1. Introduction

Mauna Kea is a dormant post-shield volcano located on the Big Island of Hawaii. The summit rises 4205 m above sea level and sits well above the typical trade-wind inversion (~2255m) that limits depth of clouds and convection within the island chain (Cao et al., 2007). Therefore, the summit is classified as semi-arid alpine tundra. At the summit, air temperatures are cool to cold, with nocturnal freezing throughout the year, and extremely dry dew-point temperatures that result in a very low density of vascular plants (James, 1922; Ugolini, 1974; da Silva, 2012).

The arid climate and low incident angle of the sun in some aspects of the Mauna Kea summit contribute to the formation of subsurface ice. Areas of permafrost were first discovered in 1969 (Woodcock, 1974). More recently Ehses (2007) measured soil temperatures in the summit area in an effort to estimate the extent of permafrost. Ehses found near surface ice at several locations that she surveyed, however, whether or not ice was present year round was not confirmed because the observing period was from mid January to early March. Nevertheless, as pertains to the ecology of the wēkiu bug, it is suggested that the sites that Ehses identified as likely to support permafrost, are not sites where wēkiu bug populations would likely be found owing to unfavorably cool temperatures.

Aside from prevailing trade winds, the summit does experience a variety of weather systems, including kona lows, upper-level lows, tropical upper-tropospheric troughs, and the rare tropical cyclone that (Blumenstock and Price, 1967; Worthley, 1967; and Kodama and Businger, 1998). These weather systems bring clouds and rain and snow to the summit.

Consistent with the nature of post-shield volcanoes, the slopes of Mauna Kea are generally smooth and gradual (on average 7-12% grade). However, on the summit, slopes of 30% can be seen on the flanks of various puʻus. Puʻus are cinder cones that were created from explosions of highly vesicular material such as ash, lapilli, and cinder. The ash was carried downwind, and the lapilli and cinder fell close to the explosion site forming the cinder cones (Porter, 1997). The current day summit geological make-up of the summit area includes an array of puʻus, glacial till, dikes, various lava flows, and glacial outwash (Wolfe et al., 1997; Sustainable Resources Group International, Inc., 2009).

The porous material that makes up the puʻu slopes is home to several plant and animal life forms. There are approximately 25 different lichen and 12 different moss communities found on the summit (Group 70 International, 2000). Mauna Kea houses a multitude of arthropods (spiders, moths, mites, spring-tails, centipedes, and true bugs). Summit life is considered an Aeolian ecosystem, which is a term first introduced by Swan (1963), that describes a habitat that is solely dependent on the transport of nutrients (biological fallout such as organic debris and insects) by the wind. Average wind speed at the summit is approximately 4-5 m s^{-1}, with much higher winds during the passage of storms (Bely, 1987; da Silva, 2012).

The Wēkiu Bug (*Nysius Wekiuicola*) has been a focus of research since its discovery in 1980 by biologists searching for insects under the Canada, France, and

Hawaii Telescope (CFHT) (Ashlock and Gagne, 1983). This true bug is endemic to the summit and receives its nutrients and moisture from the distribution of Aeolian debris and snow (Englund et al., 2002; Englund et al., 2009; Eiben and Rubinoff, 2010; Fish and Wildlife, 2010). Early entomology studies have shown that the Wēkiu Bug is most active in the winter and are commonly found in adjacent snow pack areas (Ashlock and Gange, 1983).

Although it is located in the tropics, the summit of Mauna Kea can and does receive snowfall. There are no formal studies detailing the climatology of snowfall events for the summit because of the limited snow depth and snowfall data. However, da Silva (2006) created a proxy, where observations of temperature and relative humidity are below 0°C and greater than 80%, respectively, for periods of 4 hours or more, to estimate the average number of snowfall events per month. She found that January typically has six such events, February and March both averaged five events, and November averaged four. In 2008 the summit experienced 40 days where there was recorded precipitation and temperatures below 0°C at one or more of the weather stations. In 2009 the summit experienced 52 days like this (Fig. 1).

How wind flow varies over terrain has been a widely studied (e.g., Jackson and Hunt, 1975; Whiteman, 2000). It is known that the speed, direction, and turbulence associated with wind, all change as it flows over hills. Unstable and neutrally stable air is easily carried over a hill. For stable air, the degree of stability, wind speed, and terrain characteristics determine how the protruding hills or puʻu affect the flow. The highest wind speeds in flow around a barrier are on the slopes where flow is parallel to the hills' elevation contour lines. In this study the analysis is restricted to the micrometeorology of the summit region itself (Fig. 2).

This study uses SnowModel (Liston and Elder, 2006), a spatially distributed snow evolution model, which incorporates weighted interpolations of daily weather data to derive wind-flow adjustments around the pu'u stippled summit. A description of SnowModel is given in section 2. The results of SnowModel include estimates of the distribution of snowfall and Aeolian debris, which are presented in section 3. The resulting climatological distributions are then compared with the locations where Wēkiu Bugs have been observed in the field.

2. Data and Methods

This research aims to connect previous entomological and geological studies with a micro-meteorological study of the summit. Both observations and modeling are used in hopes of gaining a better understanding of the endemic Wēkiu Bug's habitat.

2.1 Study Area

Mauna Kea is one of the five volcanoes that make up Hawaii Island. Mauna Kea's summit rises 4205 m above sea level and is located at 19.8N and -155.5W. The study area encompasses a 4320 m by 3250 m area that includes [from East to West] Pu'u Lilinoe, Puʻu Mahoe, Puʻu Kea, Puʻu Wēkiu, Puʻu Haukea, Puʻu Hau'oki, Puʻu Poliʻahu, and Puʻu Pōhaku (Fig 2). It can be seen in Fig. 2 that Pu'u Wekiu is the largest of the pu'u in areal extent and elevation difference. Elevation in the region ranges from 3741.6 m to 4205 m. The terrain is comprised mainly of cinder cones and glacial till. The central southern region of the domain is the northern tip of the Mauna Kea Ice Age Natural Area Reserve, which holds the Mauna Kea Adze Quarry.

The summit also houses the world's largest observatory for optical, infrared, and sub-millimeter astronomy. Presently, there are 13 active telescopes on the summit ridges, several which support basic weather stations (Fig. 2). Additionally, four Davis weather stations were installed in 2007 in low-lying areas within four different pu'us (Hau'oki, Kea, Wēkiu, and Pōhaku) under the supervision of the Wēkiu Bug Scientific Advisory Committee (WBSAC) (Table 1).

2.2 Model

SnowModel is a spatially distributed snow-evolution modeling system that includes first order physics required to simulate snow evolution within each of the snow climates, i.e., ice, tundra, alpine/mountain, prairie, maritime, and ephemeral (Liston and Elder, 2006). SnowModel has been tested on a variety of snowy environments (i.e., Colorado (Greene et al., 1999), Antarctica (Liston et al., 2000), Idaho (Prasad et al., 2001), and Alaska (Liston and Sturm, 2002)).

SnowModel is comprised of four sub-models, MicroMet, EnBal, SnowPack, and SnowTran-3D. MicroMet was developed by Liston and Sturm (2006b) to produce high-resolution atmospheric variables (air temperature, relative humidity, wind speed, wind direction, incoming solar radiation, incoming longwave radiation, surface pressure, and precipitation), using meteorological point data from weather stations as input. The output from MicroMet is then available as input for spatially distributed terrestrial models over a wide variety of landscapes.

Included in MicroMet is a three-step preprocessor that helps to identify and /or correct deficiencies found in the station data. MicroMet uses the Barnes objective analysis scheme (Barnes, 1973; Koch et al., 1983) to interpolate irregularly distributed meteorological data to a regularly spaced grid, with corrections based on known temperature-elevation, wind-topography, and solar radiation- topography relationships (Liston and Sturm, 2006a). Detailed physics are provided in Liston and Elder, 2006a.

EnBal uses the near-surface atmospheric conditions produced by MicroMet to simulate surface skin temperature and energy and moisture fluxes. Surface latent and sensible heat fluxes and snowmelt calculations are made using the surface energy balance model,

$$(1-\alpha)Q_{si} + Q_{li} + Q \quad + Q_h + Q_e + Q_c = Q_m \ ,$$

where Q_{si}, is the solar radiation reaching the surface, Qli is the incoming longwave radiation, Q_{le} is the emitted longwave radiation, Q_h is the turbulent exchange of sensible heat, Q_e is the turbulent exchange of latent heat, Q_c is the conductive energy transport, Q_m is the energy flux available for melt, and α is the surface albedo (Liston and Elder, 2006b). For all of the terms found in the equation, surface temperature is the only unknown, and it is solved for. Surface temperatures greater than 0°C indicate there is energy available for melting. The energy flux available for melt, Q_m, is solved by setting surface temperature to zero (Liston and Elder, 2006b).

SnowPack is a simple, single-layer, snowpack evolution model that calculates snowpack changes in response to the precipitation and melt fluxes defined by MicroMet. The compaction-based snow-density evolution is based on Anderson (1976). SnowPack uses snow temperature, overlying snow weight, and the effect of snow melting to calculate temporal snow-density changes. In the case of non-blowing snow, static-surface sublimation is calculated and used to adjust the snow pack.

SnowTran-3D simulates wind-driven snow-depth evolution over topographically variable terrain (Liston et al., 1998). There are five primary components: i) the wind-flow forcing field; ii) the wind-shear stress on the surface; iii) the transport of snow by the dominant wind-transport modes of saltation and turbulent suspension; iv) the sublimation of saltating and suspended snow; and v) the accumulation and erosion of snow at the snow surface (Fig. 3). The required model inputs include, topography, vegetation, and spatially distributed temporally variant weather data (precipitation, wind speed, wind direction, air temperature, and relative humidity).

The physics behind SnowTran-3D are primarily based on a mass-balance equation that describes the temporal variation of snow depth at each point within the simulated domain. Accumulation and erosion of snow depth at each point results from the following processes; i) changes in horizontal mass-transport rates of saltation, Q_{salt} (kg m^{-1} s^{-1}); ii) differences in horizontal mass-transport rates of turbulent suspended snow, Q_{turb} (kg m^{-1} s^{-1}); iii) sublimation of transported snow particles, Q_v (kg m^{-1} s^{-1}); and iv) the incoming rate of water equivalent precipitation, P (m s^{-1}). The mass-balance equation is

$$\frac{d(\rho_s \delta)}{dt} = \rho_w P - \left(\frac{dQ_{salt}}{dx} + \frac{dQ_{turb}}{dx} + \frac{dQ_{salt}}{dy} + \frac{dQ_{turb}}{dy}\right) + Q_V,$$

where t (s) is time; x (m) and y (m) are the horizontal coordinates in the east-west and north-south directions, and ρ_s and ρ_w (kg m^{-3}) are the snow and water densities. The mass-balance equation is solved at every time-step, for every grid cell and is coupled with neighboring cells through spatial derivatives (Liston and Sturm, 1998).

Snow drift and accumulation totals can occur by three main modes of transport (creep, saltation, suspension). Creep, the rolling motion of the snow along the surface, occurs in light wind speeds. SnowModel does not specifically state or calculate redistribution due to the creep process. Although, earlier snow redistribution studies have found that the percentage of redistribution from creep is small, between 6-10% (Kosugi et al., 1992). Saltation and suspension are the dominant processes for moving snow and the transport rate of snow by these two methods can be described by wind speed relationships.

Saltation is the transport of snow in periodic contact with and directly above the surface; transportation rate roughly increases linearly with friction velocity (Pomeroy and Gray, 1990). Whereas, suspension is the transport of snow through turbulent eddies at higher wind speeds and can occur several hundred meters above the surface. Saltation must be occurring in order to have turbulent-suspended snow particles (Liston and Sturm, 1998). Liston and Sturm (1998) showed that at higher frictional velocities, suspension is the dominant mode of transport over saltation.

To allow the initial processes that allow snow to be transported, the snow depth must surpass the vegetation holding depth and break the gravitational and cohesive bond of the ice crystals. Vegetation holding depth is defined as the height that the snowfall accumulation must exceed to cover various surface characteristics, which may include grass, boulders, and other features blocking snow's path. Along with exceeding the vegetation holding depth, a threshold friction velocity (u*t) must be exceeded to lift the snow for transport. The shear stress on the surface, u* (friction velocity), produced by the wind is the main determining factor for transport. It is defined by,

$$u_* = u_r \frac{\kappa}{\ln \frac{z_r}{z_0}},$$

where u_r (m s^{-1}) is the wind speed at reference height z_r (m), z_0 (m) is the surface roughness length, and κ is von Karman's constant. The friction velocity of a given wind must exceed a threshold friction velocity value (u*t) for transport to begin. The threshold friction velocity is lower (u*t = 0.07-0.25 m s^{-1}) for fresh, loose, dry snow and during snowfall and higher (u*t = 0.25-1.0 m s^{-1}) for older, wind hardened, dense, and/or wet snow where inter-particle bonds and cohesion forces are strong (Kind, 1981).

The loss of snow particle mass as a result of sublimation is a function of wind speed, air temperature, humidity, particle size, and solar radiation. Sublimation is the cause for significant reductions in snow mass in snow accumulation areas (Schmidt, 1982; Marsh, 1999).

To estimate the bug fall distribution on the summit of Mauna Kea, we assumed a constant bug fall rate and allowed SnowModel to determine the final bug fall distribution based on the input of wind data from 2008 to 2010 from the summit weather stations. To model the bug fall, only Micromet and SnowTran-3D sub-models are used. The SnowPack and EnBal sub-models are turned off, to eliminate melting and density changes from energy inputs to the modeled bug fall. Within the SnowTran-3D sub-model, sublimation is removed as a valid process of snow transport and is set to zero. The elimination of sublimation, evaporation, and melting of the solid matter bug fall is consistent with the notion that bug fall mass is not lost to the atmosphere during transport or when settled. To imitate the transport of solid bug fall matter at the summit, temperature, relative humidity, and a bug fall precipitation rate were set to constant values of 0°C, 100%, and 0.2 mm hr^{-1}, respectively. Hypothetical bug fall stations were created at ten locations around the perimeter of the study domain. The ten stations acted to provide steady bug fall data, as listed above, for ingest into MicroMet. The bug fall precipitation rate (0.2 mm hr^{-1}) is a hypothetical value based on a rate that would allow for viewable model return. The results from this modeling exercise only give a relative distribution field for bug fall, but not absolute values for accumulation, since data on bug-fall rates are unavailable.

Studies from Eiben and Rubinoff (2010) and Ashlock and Gagne (1983) suggest the Wēkiu Bug feeds on dead or dying insects, which are all wind driven and deposited on the summit from lower elevations. This study does not incorporate flight dynamics of the insects and bugs found within bug fall on the summit; it is assumed the majority of the incoming bug fall is dead and did not use its own means for transport or flight once at summit level.

3. RESULTS

3.1 Case Study

Initial testing of SnowModel was completed after the passage of a cold front on 11 January 2011. Between 21:30 UTC 11 January and 0000 UTC 12 January 2011, a field experiment on the summit measured the fallen and drifted snow in Pu‘u Wēkiu and Pu‘u Hau‘oki. The cold front dropped ~15 cm of snow (Fig. 4) with drifts up to 60 cm on the summit. Summit temperature, relative humidity, wind speed and direction, and precipitation observations from January 2011 were used as input for SnowModel (Fig. 5). The majority of the winds during the event were from the west and southwest (Fig. 5d).

Snow depth measurements took place between 2130 UTC 11 January and 0000 UTC 12 January 2011; and focused on the center depressions and the interior slopes of Pu’u Wēkiu and Pu’u Hau’oki. Measurements from the field experiment on 11 January 2011 are compared against SnowModel output from 10 January 2011. The bulk of the snowfall associated with the frontal passage occurred on 10 January 2011.Output from SnowModel for 0959 UTC 11 January 2011 shows an average depth of ~15 cm covering a majority of the summit, in good agreement with observed snow depth (Fig. 6).

The overall spatial pattern of the modeled snowfall for 10 January 2011 is in reasonable agreement with snow depth observations within Pu’u Wēkiu and Pu’ Hau’oki. Field observations show snow depth values increasing along the inner western slope of Pu’u Wēkiu, with the shallowest recordings in the center. This same spatial gradient is captured within the modeled output for Pu’u Wēkiu. However, the model does show a tendency to overestimate, especially with the depression of the pu’u and does not extend the higher snow accumulation down the inner western slope. The inner western slope of Pu’u Wēkiu, in this case study, is considered to be the leeward side on the western crest of Pu’u Wēkiu. Discrepancies between the model and the observations in this case may be, in part, caused by the limited number and spatial layout of the weather stations, leading to variations in wind and precipitation. The model interpolates point data to a gridded field. The buildup of snow along the upper section of the inner western slope, suggests that the modeled wind speed is dropping more quickly than is actually occurring.

Within Pu‘u Hau‘oki, the overall spatial pattern from the model and observations again were in reasonable agreement. In the western crease of the pu'u center, the model did a fair job in representing actual snow depths. The model underestimates the inner northern slope of the pu‘u, but is in agreement with the increase in snow depth that is occurring spatially, which also holds true for the inner western slope. Pu’u Hau’oki is shielded from the south and west by other pu’us and observatories, more so than Pu’u

Wēkiu. The sharp gradient found in the snow accumulation in Pu'u Wēkiu is not seen here, due to the less noticeable wind acceleration and the less steep slope within this pu'u.

Although, the overall spatial patterns from the model are in agreement with the observations, some variability in the snow depth observations not captured by the model can be, in part, attributed to the limited number of weather stations within the study domain. Additionally, subgrid-scale variability in surface terrain and roughness elements will lead to discrepancies between model and observations. The model's output resolution and 1/3 arc-second National Elevation Dataset (NED) input, are not sufficient to resolve individual boulders that cause variations across the snow-depth field. GPS receivers were used to point locate the snow depth observations, while the model uses the longitude and latitude locations from NED input.

3.2 Wind and snowfall observations

Wind and precipitation data (Figs. 1, 7 and 8) are used in daily model runs to estimate the climatological accumulation of snowfall and bug fall across the summit region. Snow events are characterized by days that have precipitation and the summit average temperature is freezing or below. An overview of the wind and precipitation data is presented here. Nominally, the wind speed threshold for saltation is 5 m s^{-1} and the threshold for suspension is 15 m s^{-1} (Liston and Sturm, 1998).

Easterly winds prevail in snow events for 2008, especially in February, March, and November (Fig. 7a). December snow events are governed by both easterly and westerly winds; the same goes for snow events in April. The summit received snowfall 40 days out of the year for 2008 (Fig. 1a). The annual total snowfall observed for the year averaged over all the observation sites was 193 mm.

Winds during snow events for 2009 are predominantly westerly (Fig. 7b). January, March, and November have the greatest variation in snow event wind direction. In November there are a number of events with average winds being northerly. In January and March there are a number of snow events having easterly winds. The higher percentages of northeasterly and southeasterly winds are not seen during snow events for 2009, as they were in 2008. Winds with strong northern and southern directions are also less frequent during snow events. Snowfall on the summit was recorded during 52 days out of the year for 2009 (Fig. 1b) and the annual total snowfall observed for the year averaged over all the observation sites was 239 mm. Due to equipment failures, precipitation measurements from 2010 were limited.

In this study it is suggested that bug fall accumulation patterns are governed by similar physics as snow transport. In estimating the long-term climatology of the bug fall distribution, wind data (Fig. 8) and model results throughout the period of study were integrated.

In overview, analysis of all the summit surface winds for the period of study, 2008 through 2010, shows that winds favor easterly and westerly directions. The summit experiences winds with easterly components 59% of the time, with a westerly component 41% of the time (Fig. 8). Southerly and northerly winds occur relatively infrequently and tend to be lighter. In total summit winds greater than 10 m s^{-1} occurred 31% of the time. Stronger winds favor southwesterly and eastnortheasterly directions (Fig. 8).

3.3 Impact of summit puʻus on wind speed and direction

MicroMet was run to model the changes that occur to winds as they interact with the puʻu stippled summit. Cardinal and inter-cardinal (north, south, east, west, northeast, southeast, southwest, and northwest) wind fields of 7 m s^{-1} were initialized into MicroMet to display how the pu'us affect winds from a given direction (Figs. 9-10). Puʻu Wēkiu had the greatest impact on the wind field for all eight directions. Winds with easterly components have the greatest positive wind speed changes on the puʻu (Fig. 9a). The outer eastern slope of Puʻu Wēkiu for these three scenarios (east, northeast, southwest) saw an increase in wind speeds by ~20%.

For both direct west and east winds, Puʻu Wēkiu caused more winds to flow south than north around the pu'u around the pu'u judging from wind directional changes (Fig. 10). Puʻu Hauʻoki does not exhibit any great speed changes, however, approaching winds with a westerly component experience a greater directional change than winds with an easterly component (Fig. 10). Wind speed changes due to interaction with Puʻu Haukea are most recognizable from winds that have north and east components. The increase, however, is not as distinct as seen on Puʻu Wēkiu. Consistent with expectations, the center depressions for all three puʻus experience wind speeds that are ~40% slower than surrounding winds.

3.4 SnowModel Climatology

Wind and precipitation data for 2008 and 2009 (Figs. 1 and 7) are used in model runs to estimate the climatological distribution of snowfall accumulation across the summit region. For the snowfall estimation, the model is run with wind data during snow events only (Fig. 7). Precipitation data for 2010 are incomplete as a result of instrumentation issues. Therefore, the results for 2010 are not included in the snowfall climatology.

Accumulated snowfall and bug fall patterns agree well (Figs. 11-12), with the maxima in accumulated snow and dead bugs on the lee sides of ridges and crests. Lower accumulation areas are seen on the windward sides in areas of enhanced winds, where saltation and scouring are active (Figs. 11-12). Differences in the patterns of bug fall and snowfall accumulation are consistent with differences in the dominant wind direction over the days of integration.

Pu‘u Haukea’s maxima for snowfall and bug fall consistently occur on the outer southern and southeastern slopes (Figs. 13a and 14a). A second snowfall maximum is seen on the inner northeastern slope of Pu‘u Haukea.

Pu‘us Poli‘ahu and Pōhaku display similar patterns for snowfall and bug fall (Figs. 13b and 14b). Maxima are seen on the southern slopes of Pu‘u Pōhaku and Pu‘u Poli‘ahu. The maxima associated with the lateral ridges on the southwest slope of Pu‘u Poli‘ahu are well defined. Pu‘u Wēkiu and Pu‘u Hau‘oki clearly show the effect that wind direction and speed have on accumulation locations for both snow and bug fall (Figs. 13b and 14b). Maxima on Pu‘u Wēkiu are seen on both the inner and outer eastern slope and on either side of the ridge extending north from the pu‘u. The higher values on the eastern slopes are the product of the higher westerly wind speeds observed in 2009. The outer southern slope in both easterly and westerly winds accumulates maxima on Pu’u Wēkiu.

4. Conclusions and Discussion

The summit of Mauna Kea is an Aeolian system, where nutrients primarily come from matter being blown in from lower elevations. The cinder cone (pu'u) stippled summit area affects local wind patterns and summit deposition of moisture and nutrients, which is of great interest in understanding the life cycle, habitat, and distribution of the Wēkiu Bug and other summit species. Pu'us protrude as much as 200 m above the surrounding surface elevations, creating slope angles of ~30% grade. In general, winds traveling up hills or pu'us and on the ridge are faster than those over flat terrain and within the pu'u center. Wind that travels parallel to the slope gradient also experiences increases in speed. On the down-slope sides, winds speeds tend to decelerate. As the wind approaches the pu'us, it is forced around or over the pu'u.

For the summit of Mauna Kea winds with an easterly or northerly direction produce the greatest acceleration in wind speed, especially on Pu'u Wēkiu, the largest cinder cone. Consequently, the maxima in accumulated snow and dead bugs are seen on the lee sides of ridges and crests where deposits are made as the wind falls below the thresholds for suspension or saltation. Areas like Pu'u Haukea and Pu'u Poli'ahu have the greatest snowfall accumulation on their southern outer slopes, with maxima occurring where the parallel gradient curves. The summation of the years creates a smoother gradient of snow along the slope, as the percentage of east to west winds between the two years becomes comparable.

In this study it is suggested that the maximum bug-fall accumulation patterns are governed by similar physics as snow transport, with allowance made for the fact that dead bugs do not change phase. The modeled maxima in bug-fall accumulation is located on the leeward sides of the pu‘us and the position of the maxima is controlled by wind speed, much like that of the snowfall accumulation. The case study suggests that the model may have a tendency to underestimate the wind speed and snow may actually extend further down the slope on the leeward side. As expected, lower accumulation is seen on the windward sides in areas of enhanced winds, where saltation and scouring are active.

4.1 Specific conclusions

- ❖ The center depressions for the three main pu’us experience wind speeds that are ~40% slower than surrounding winds.
- ❖ Prevailing easterlies have maximum moisture and nutrient accumulations on the inner eastern slope and the outer western slope on Pu‘u Wēkiu and the ridge extending north from the pu’u. The highest nutrient concentrations are towards the upper portion of the slope. Stronger winds cause nutrients to also accumulate on the outer northwestern slope of Pu‘u Wēkiu.
- ❖ Prevailing westerlies allow for moisture and nutrients to collect along the inner western slope of Pu‘u Wēkiu. Moisture and nutrient accumulation is the greatest on the outer eastern slope of Pu‘u Wēkiu, with the nutrient maxima accumulating half way up this side. Additionally, the eastern slope of the ridge extending from Pu‘u Wēkiu traps nutrients on the upper portion of the slope.
- ❖ Pu‘u Pōhaku’s maxima of nutrients and moisture occur on the outer southern slope. There is a second bug fall maxima on the western slope.
- ❖ Nutrient and moisture supplies on Pu‘u Haukea are the greatest on the outer southern

and southeastern slopes and the inner northwestern slope.

- Maximum moisture on Pu‘u Poli‘ahu is found continuously down the outer southern slope. Nutrient accumulation occurs mainly on the upper section of the outer southern slope. Down the inner northern slope, nutrient and moisture maxima occur.
- Nutrient accumulation on Pu‘u Hau‘oki is minimal, with moisture accumulation occurring on the outer southern slope.

4.2 Discussion

The synoptic-scale winds on the summit are mainly controlled by the prevailing surface high-pressure center that is located north of the Hawaiian Islands and the position of the polar jet stream and its storm track, which shifts southward in winter. When the high pressure dominates, the winds favor easterly directions, and when the jet stream expands near Hawaii, the winds turn westerly. The location of both the high and the jet are influenced by ENSO. On the local scale the variable terrain of the surface alters the free atmosphere wind significantly.

The summit is an Aeolian system, where nutrients primarily come from matter being blown to the summit from lower elevations. Areas of deposits differ with changing wind speeds and directions. The strength of the wind is important in determining how much snow and nutrient is carried and where it is eventually deposited. An increase in wind speed increases the saltation and turbulent suspension and results in the moisture and nutrient maxima to accumulate further down the slope of an associated pu'u. Slope angle and aspect have primary effects on wind speed and direction, and subtle secondary effects on the accumulation patterns.

The variables used to simulate incoming bug fall are hypothetical and are set at the minimum solid precipitation value for the model to run. It is suggested that since wind is the primary agent of debris transportation, climatological patterns for bug-fall accumulation would likely follow the patterns seen in the model analysis presented here.

Limited bug-fall data suggest that the primary source for the bug fall is from the tundra and brush areas just below the summit area and above the tree line, with some additional bugs coming from agricultural areas further from the summit (Jesse Eiben, personal communication). For modeling purposes, it was assumed that the background bug fall from these areas was initially evenly distributed. Time-series data on bug fall with analysis of the taxonomy and source of the bugs are not available. Comprehensive bug-fall data are very time consuming and expensive to obtain. So at present there is no way to validate the bug-fall model results quantitatively. Nevertheless, we argue that the bug-fall results are of interest, because they provide a potentially useful guide to entomologists in the field working to locate wēkiu bug populations.

The rotation of synoptic wind from prevailing easterlies (summer) to more variable easterlies and westerlies (winter) affects accumulation patterns on the summit, with the greatest differences occurring on Puʻu Wēkiu. Western wind regimes deposit most nutrients on the outer eastern slopes of the puʻu, whereas, during easterly wind regimes the outer western and the inner eastern slopes of Puʻu Wēkiu accumulate the most nutrients. Nutrients are found on the outer southern slope of Pu'u Wēkiu in both easterly and westerly winds, and the wind flows along the slopes gradient.

Bug fall and snowfall fields show similar characteristics where accumulations occur, but the fields are not exact replicas due to the different set of days used in the integration. The bug fall accumulations were modeled using winds from the entire three-year period. For snowfall, only the winds that were present during snow events were used to distribute snowfall on the summit. Also, sublimation and melting are ignored when modeling bug fall; there are no losses to the maxima accumulations through phase changes. Nutrient maxima occur in clumped areas, while snowfall accumulation areas are more continuous down the slope. This clumping of maxima bug-fall areas may arise from the uniform size distribution of the bug fall and the way in which cohesion and friction velocities where calculated in the model. The constant 0°C air temperature used during bug fall modeling resulted in a “stickier” surface, which may have promoted clumping.

4.3 Relation to Wēkiu Bug Ecology

Several field surveys have helped to identify the locations favorable for Wēkiu Bug habitat through various trapping techniques (Brenner, 2006; Englund et al., 2002; Englund et al., 2009; Eiben and Rubinoff, 2010). Wēkiu Bugs have been recorded on the west and northwest rim of Pu’u Haukea, in the flatter area between Pu’u Haukea and Pu’u Poli’ahu, on the northern side of Pu’u Hau’oki and on the southern and eastern rim, on the outer western slope of Pu’u Wēkiu, in the Pu’u Wēkiu center depression, on the inner eastern slope of Pu’u Wēkiu, and on the outer eastern slope of Pu’u Wēkiu and the ridge extending from the pu’u (Figs. 11-12).

The annual Wēkiu Bug field surveys led by Brenner (2006) from 2002 to 2006, found the highest count of Wēkiu Bugs in the spring. These field surveys were conducted on Pu‘u Hau‘oki and Pu‘u Wēkiu. The most sampling has been done on Pu‘us

Hau‘oki, Haukea, and Wēkiu. Englund et al. (2009) sampled a pu‘u around the Very Long Baseline Array (VLBA) on Mauna Kea in both 2007 and 2008. The north side of the pu‘u only positively observed one Wēkiu Bug between 2007 and 2008. The south side positively observed eleven and nine Wēkiu Bugs in 2007 and 2008. The sample sites on Pu‘us Hau‘oki, Haukea, Wēkiu had considerably more Wēkiu Bug activity than the pu‘u by the VLBA. Englund et al. (2009) compiled Wēkiu Bug sample site data from 2001 to 2008 showing that 822 Wēkiu Bugs have been observed on Pu’u Haukea over that 9-year period.

Englund et al. (2009) observed 537 Wēkiu Bugs using 42 traps located on Pu‘u Haukea, Pu‘u Hau‘oki, Pu‘u Wēkiu, and surrounding the pu‘u by VLBA in 2007. The traps for 2007 had a total trap day number of 252. In 2008, their observations of Wēkiu Bugs were ~7x less than observed in 2007. In 2008, 30 traps in approximately the same summit locations counted 70 Wēkiu Bugs. The 2008 study had a total trap day value of 120.

The model output shows that the locations of the Wēkiu Bug recordings and trappings, except for the area between Pu‘u Haukea and Pu‘u Poli‘ahu and the center depression of Pu‘u Wēkiu, receive high amounts of snowdrift over the winter season. The locations that receive high snowdrifts also accumulate the highest density bug fall, except for Pu‘u Hau‘oki. Bug fall accumulation is considerably less on Pu‘u Hau‘oki than Pu‘u Haukea or Pu‘u Wēkiu.

The pu‘us are cinder cones and are made up of ash, lapilli, and cinder from explosions that occurred on the summit. This combination of volcanic rock allows for large interspatial areas between rocks to occur, a necessity for the Wēkiu Bug. The majority of the land surrounding the pu'us is comprised of older hawaiite-mugearite lava flows, which is primarily made up of ʻa'ā lava with large rough sections. The geological make-up surrounding Puʻu Pōhaku's base is primarily glacial till, as well as the eastern side of Puʻu Wēkiu. The finer make up of glacial till is unsuitable for Wēkiu Bug life (Englund et al., 2002; Eiben and Rubinoff, 2010).

The pu'us on the summit act to speed up and slow down winds, change their direction, and thereby act as a trap for moisture and nutrients being blown on the summit. Concurrently, the pu'us are, generally areas with high interstitial spaces (like cinder), which is the preferred habitat for the Wēkiu Bug. The combination of moisture, nutrients, and cinder substrate is presumably where the population of Wēkiu Bugs will be found. Previous trapping locations support this suggestion (Figs. 11 and 12). It is hoped that the results of the snow and bug-fall climatology presented in this paper will be of value to entomologists and biologists in their efforts to better understand and characterize the fragile ecology of the summit area of Mauna Kea.

5. Acknowledgements

Foremost, we are indebted to Dr. Glen Liston for give us access to his SnowModel and for his helpful comments and support throughout this research. We are grateful to Sara da Silva for help with data analysis tools. Thanks go to Ryan Lyman for his efforts in siting and collecting the Davis weather station data. Ryan, along with Chris Chambers and Matt Foster helped to collect case snow depth measurements. This research was supported by the Office of Mauna Kea Management.

6. References

Anderson, E.A., 1976: A point energy and mass balance model of a snow cover. NOAA Technical Report NWS-19, 150 pp.

Ashlock, P., and Gagne, W., 1983: A remarkable new *Micropterous Nysius* species from the aeolian zone of Mauna Kea, Hawaii Island (Hemiptera: Lygaeidae). *International Journal of Entomology.,* 25: 47–55.

Barnes, S. L., 1973: Mesoscale objective analysis using weighted time-series observations. NOAA Tech Memo. ERL NSSL-62, National Severe Storms Laboratory, Norman, OK 73069, 60 pp. [NTIS-COM-73-10781].

Bely, P.-Y., 1987: Weather and seeing on Mauna Kea. *Publications of the Astronomical Society of the Pacific*., 99: 569–570.

Blumenstock, D.I., and Price, S., 1967: Climates of the States: Hawaii. Climatology of the US, No. 60-51. US Department of Commerce, 27 p.

Cao, G., Giambelluca, T. W., Stevens, D. E., and Schroeder, T. A., 2007: Inversion variability in the Hawaiian trade wind regime. *Journal of Climate*., 20: 1145–1160.

Conant, S., 2007: Memorandum: Climate variability and microscale ecology of Mauna Kea study. [Between Mauna Kea Management Board and Wēkiu Bug Scientific Advisory Committee].

da Silva, S. C., 2006: Climatological analysis of meteorological observations at the summit of Mauna Kea. OMKM Technical Report, Dept. of Meteorology, University of Hawaii at Mānoa, 77 pp. [Available at: www.mkwc.ifa.hawaii.edu/archive.]

da Silva, S. C., 2012: High altitude climate of the Island of Hawai'i. MS Thesis, Dept. of Meteorology, University of Hawaii at Mānoa, 110 pp. [Available at http://www.soest.hawaii.edu/MET/Faculty/businger/highlights.html.]

Eiben, J., and Rubinoff, D., 2010: Life history and captive rearing of the Wēkiu bug (*Nysius Wēkiuiucola*, Lygaeidae), an alpine carnivore endemic to the Mauna Kea volcano of Hawaii. *Journal of Insect Conservation.,*14: 701–709.

Englund, R. A., Polhemus, D. A., Howarth, F. G., and Montgomery, S. L., 2002: Range, habitat, and ecology of the Wēkiu Bug (*Nysius Wēkiuicola*), a rare insect species unique to Mauna Kea, Hawaii Island. Report prepared for Office of Mauna Kea Management, University of Hawaii at Hilo, 200 W. Kawili Street, Hilo, HI 96720.

-----, Preston, D. J., Vorsin, A. E., Evenhuis, N. L., Myers, S., and Englund, L. L., 2009: Results of the 2007-2008 alien arthropod species and Wēkiu bug monitors on Mauna Kea, Hawaii Island. Hawaii Biological Survey final report prepared for Office of Mauna Kea Management, University of Hawaii at Hilo, 200 W. Kawili Street, Hilo, HI 96720.

Ehses, J., 2007: GIS-gestützte Abschätzung möglicher Permafrostvorkommen am Mauna Kea, Hawaii, mittels klimageographischer Modellierung. M.A. Thesis, Department of Geography and Climate, Rheinisch-Westfälische Technische Hochschule University – Aachen, 106 pp.

Fish and Wildlife Service, 2010: Endangered and Threatened Wildlife and Plants; Review of Native Species That are Candidates for Listing as Endangered or Threatened; Annual Notice of Findings on Resubmitted Petitions; Annual

Description of Progress on Listing Action. 50 CFR Part 17 [Docket No. FWS-R9-ES-2010-0065;MO-9221050083-B2].

Greene, E. M., Liston, G. E., and Pielke, R. A., Sr., 1999: Simulation of above treeline snowdrift formation using a numerical snow-transport model. *Cold Regions Science and Technology,* 30: 135–144.

Group 70 International, 2000: Mauna Kea Science Reserve Master Plan: A final environmental impact statement Master Plan. Report prepared for Research Corporation of the University of Hawai'i by Group 70 International, 925 Bethel Street, 5th Floor. Honolulu, HI 96813.

Jackson, P. S and Hunt, J. C. R., 1975: Turbulent wind flow over a low hill. *Quarterly Journal of the Royal Meteorological Society,* 101: 929–955.

Kind, R. J., 1981: Snow drifting. *Handbook of Snow, Principles, Processes, Management, and Use.* D.M. Gray and D.H. Male, Editors, Pergamon Press, p. 338-359.

Koch, S. E., DesJardins, M., and Kocin, P. J., 1983: An interactive Barnes objective map analysis scheme for use with satellite and conventional data. *Journal of Climate and Applied Meteorology,* 22: 1487–1503.

Kosugi, K., Nishimura, N., and Maeno, N., 1992: Snow ripples and their contribution to the mass transport in drifting snow. *Boundary Layer Meteorology,* 59: 59-66.

Kodama, K. R., and Businger, S., 1998: Weather and forecasting challenges in the Pacific region of the National Weather Service. *Weather and Forecasting*., 13: 523–546.

Liston, G. E., Haehnel, R. B., Sturm, M., Hiemstra, C. A., Berezovskaya, S., and Tabler, R. D., 2007: Simulating complex snow distributions in windy environments using SnowTran-3D. *Journal of Glaciology*, **53**, 241-256.

-----, and Elder, K., 2006a: A meteorological distribution system for high-resolution modeling (MicroMet). *Journal of Hydrometeorology.,* 7: 217–234.

-----, and Elder, K., 2006b: A distributed snow-evolution modeling system (SnowModel). *Journal of Hydrometeorology.,* 7: 1259–1276.

-----, Haehnel, R. B., Sturm, M., Hiemstra, C. A., Berezovskaya, S., and Tabler, R. D., 1998: Instruments and methods, Simulating complex snow distributions in windy environments using SnowTran-3D. *Journal of Glaciology,* 53: 241–256.

-----, and Sturm, M., 1998: A snow-transport model for complex terrain. *Journal of Glaciology.,* 44: 498–516.

-----, and -----, 2002: Winter precipitation patterns in arctic Alaska determined from a blowing snow model and snow-depth observations. *Journal of Hydrometeorology,* 3: 646–659.

-----, and -----, 2006: A meteorological distribution system of high-resolution terrestrial modeling (MicroMet). *Journal of Hydrometeorology,* 7: 217–234.

-----, Winther, J.-G., Bruland, O., Elvehoy, H., Sand, K., and Karlof, L., 2000: Snow and blue-ice distribution patterns on the coastal Antarctic ice sheet. *Antarctic Science,* 12: 69–79.

Pomeroy, J. W., and Gray, D. M., 1990: Saltation of snow. *Water Resources Research,* 26: 1583–1594.

Porter, S. C., 1997: Late Pleistocene eolian sediments related to pyroclastic eruptions of Mauna Kea Volcano, Hawaii. *Quaternary Research.,* 47: 261–276.

Prasad, R., Tarboton, D. G., Liston, G. E., Luce, C. H., and Seyfried, M. S., 2001: Testing a blowing snow model against distributed snow measurements at Upper Creek, Idaho, United States of America. *Water Resources Research,* 37: 1341–1350.

Swan, L., 1963: Aeolian zone. *Science,* 140: 77–78.

Schmidt, R. A, 1982: Vertical profiles of wind speed, snow concentration, and humidity in blowing snow. *Boundary Layer Meteorology,* 23: 223–246.

Sustainable Resources Group International, Inc., 2009: Natural resources management plan for the UH management areas on Mauna Kea: A sub-plan of the Mauna Kea Comprehensive Management Plan. Prepared by the Sustainable Resources Group Internationals, Inc.,111 Hekili Street, Suite A373, Kailua, HI, 98734.

Ugolini, F. C., 1974: Hydrothermal origins of the clays from the upper slopes of Mauna Kea, Hawaii. *Clay and Clay Minerals,* 22: 189–194.

Whiteman, C. D., 2000: *Mountain Meteorology—Fundamentals and Applications.* New York: Oxford University Press.

Wolfe, E. W., Wise, W. S., and Dalrymple, G. B., 1997: The geology and petrology of Mauna Kea Volcano, Hawaii – A study of post shield volcanism. *U.S. Geological Survey Professional Paper,* 1557, pp. 143.

Woodcock, A. H., 1974: Permafrost and climatology of a Hawaii volcano crater. *Arctic and Alpine Research*, 6: 49–62.

Worthley, L. E., 1967: Weather phenomena in Hawaii. Part 1. Synoptic climatology of Hawaii. Hawaii Institute of Geophysics, University of Hawaii, 40 pp. [Available from Dept. of Meteorology, University of Hawaii, 2525 Correa Rd., Honolulu, HI 96822.]

7. Tables

TABLE 1

Station	Lat (N)	Long. (W)	Elev. (m)	T (°C)	RH (%)	WS (m/s)	WD (°)	Precip. (mm/hr)	Valid Dates
MKD Hau'oki	19.8267	-155.4753	4138	X	X	X	X	X	01/2008 – 03/2009 05/2009 – 07/2009 10/2009 - 7/2010
MKD Wekiu	19.8192	-155.4697	4153	X	X	X	X	X	01/2008 04/2008 – 04/2009 09/2009 -03/2010 05/2010- 07/2010
MKD Kea	19.8261	-155.4683	4168	X	X	X	X	X	01/2008 – 01/2009
MKD Pohaku	19.8253	-155.4900	4003	X	X	X	X	X	01/2008 – 04/2008
UH88	19.8230	-155.4694	4214	X	X	X	X	X	01/2008 – 01/2011
CFHT	19.8253	-155.4688	4204	X	X	X	X		01/2008 – 07/2009 09/2009 – 01/2011
JCMT	19.8228	-155.4770	4075	X	X	X	X		05/3008 – 01/2011
UKIRT	19.8224	-155.4703	4199	X	X	X	X		01/2008 – 01/2011
SUBARU	19.8255	-155.4760	4163	X	X	X	X	X	01/2008 – 02/2008 05/2008 – 01/2011
VLBA	19.8014	-155.4555	4077	X	X	X	X	X	01/2008 – 01/2011
IRTF	19.8262	-155.4720	4168	X	X	X	X		01/2008 – 01/2011
SMA	19.8242	-155.4782	4080	X	X	X	X	X	01/2008 – 03/2008 05/2008 – 12/2008 07/2010 – 01/2011

Table 1: Weather stations and their locations, elevations, recorded variables, and valid dates for this study. Abreviations in the table include: Mauna Kea Davis stations (MKD), University of Hawaii 88" Telescope (UH88), Canada, France, Hawaii Telescope (CFHT), United Kingdom Infra Red Telescope (UKIRT), James Clark Maxwell Telescope (JCMT), Very Long Baseline Array (VLBA), Infra Red Telescope Facility (IRTF), and Sub-Millimeter Array (SMA).

7. Figures

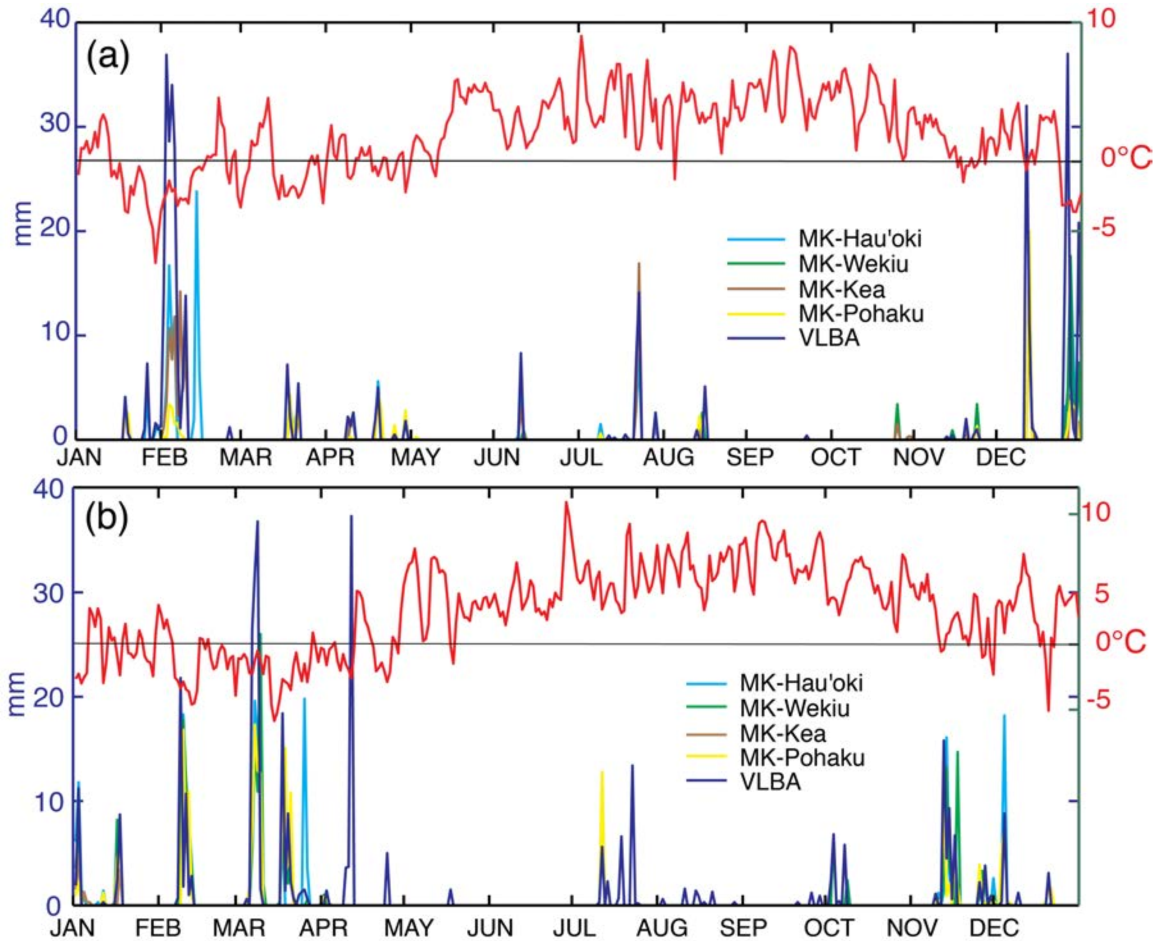

FIGURE 1. Time series of summit precipitation (mm) from listed weather stations and average daily temperature (°C, in red) from the United Kingdom Infra-Red Telescope (UKIRT) for a) 2008; b) 2009.

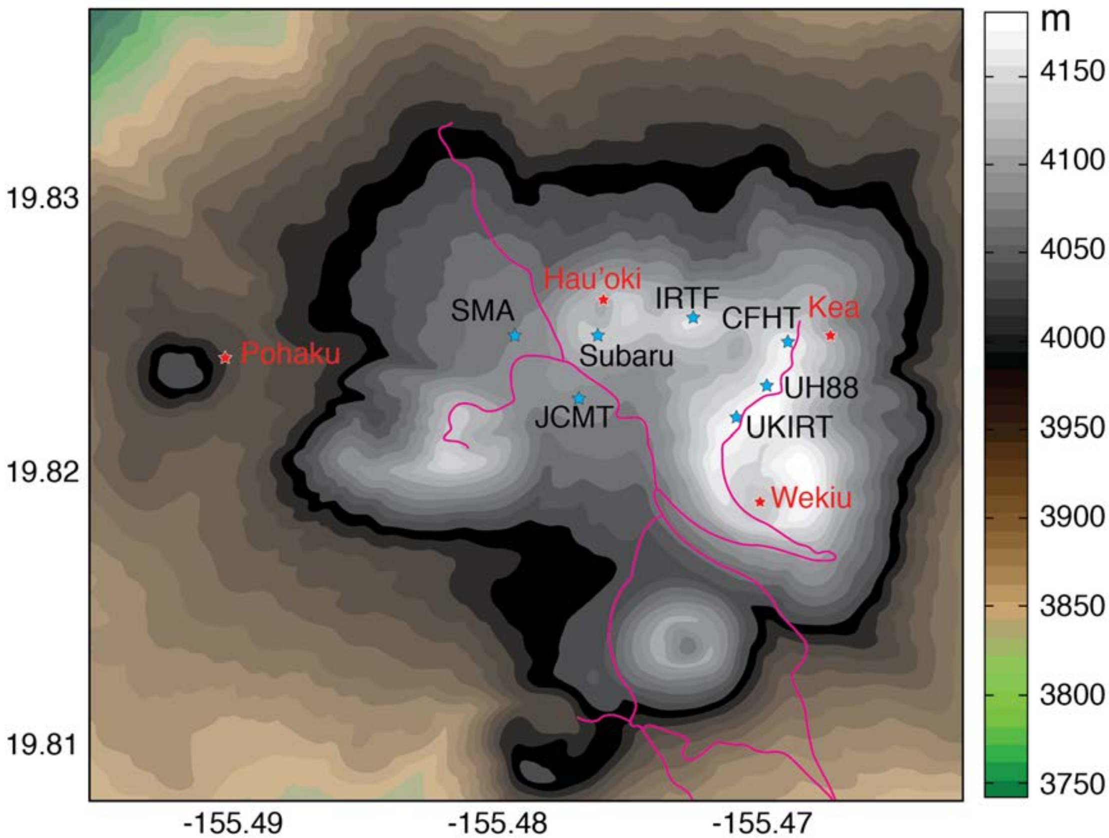

FIGURE 2. Study area spans from 19.808 N to 19.837 N and -155.495 W to -155.455W, a 140400 m^2 area. Plotted are locations of Davis weather stations (red) and telescope weather stations (blue). See Table 1 for locations and definitions of acronyms.

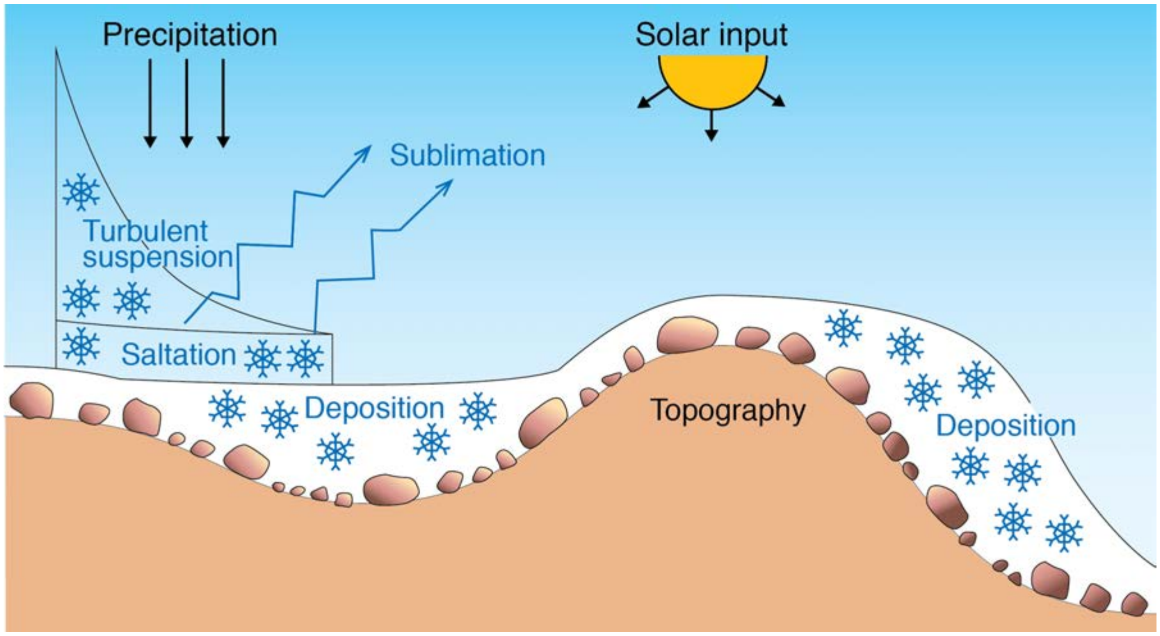

FIGURE 3. Key features of the snow-transport model (after Liston et al., 2007)

FIGURE 4. Field experiment on 11 JANUARY 2011; a) Pu‘u Hau‘oki during field experiment, taking snow depth measurements (Photo by C.R.S. Chambers); b) ruler showing depth in cm (Photo by L. Eaton).

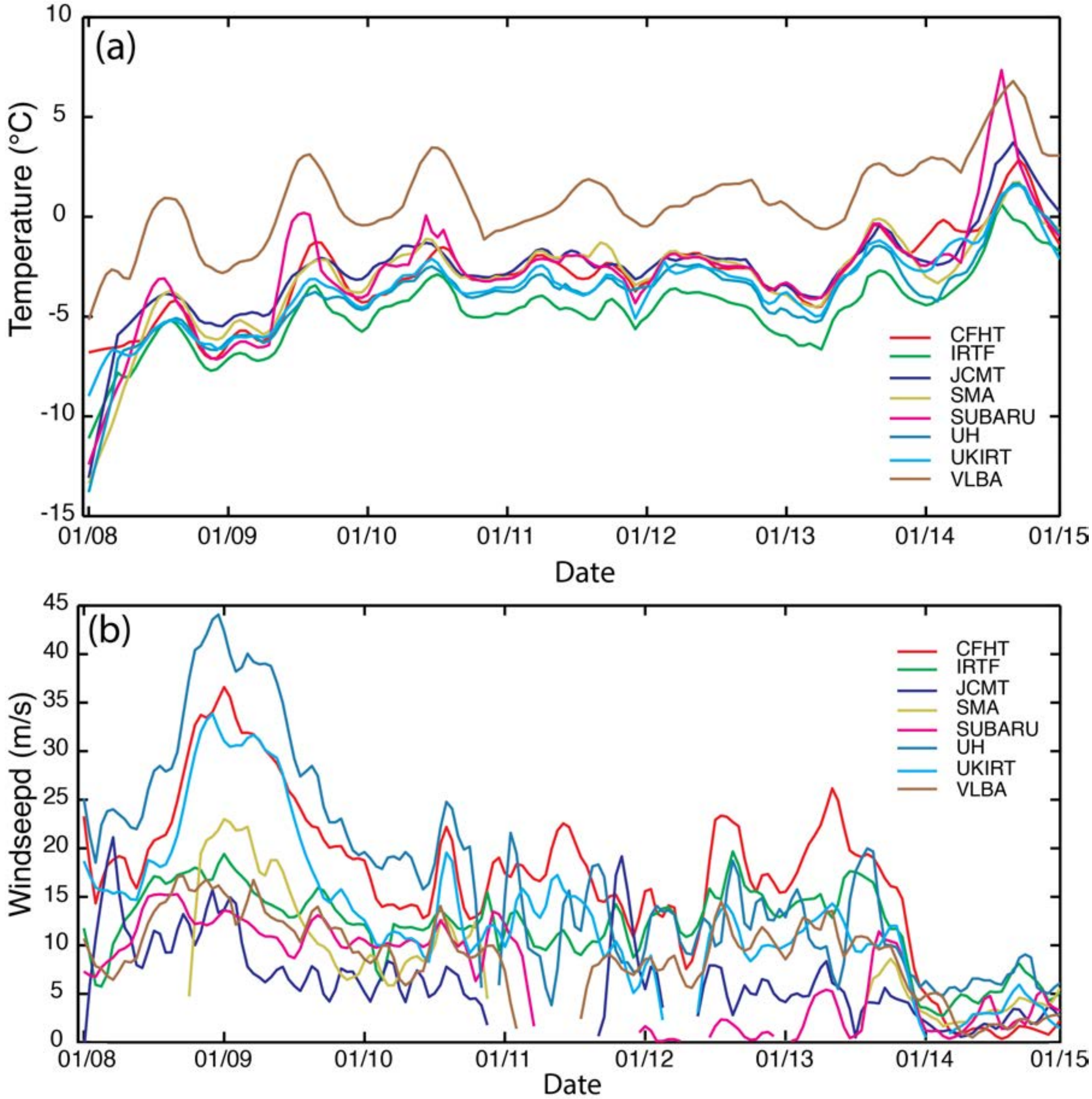

FIGURE 5. Mauna Kea summit a) average hourly temperatures and b) average daily wind speed for 8-14 January 2011. c) Precipitation time series for 12 UTC 09 January to 2300 UTC 11 JANUARY 2011. d) Wind rose plot of Mauna Kea summit wind speeds and directions from 1000 UTC 09 January to 0900 UTC 11 JANUARY 2011.

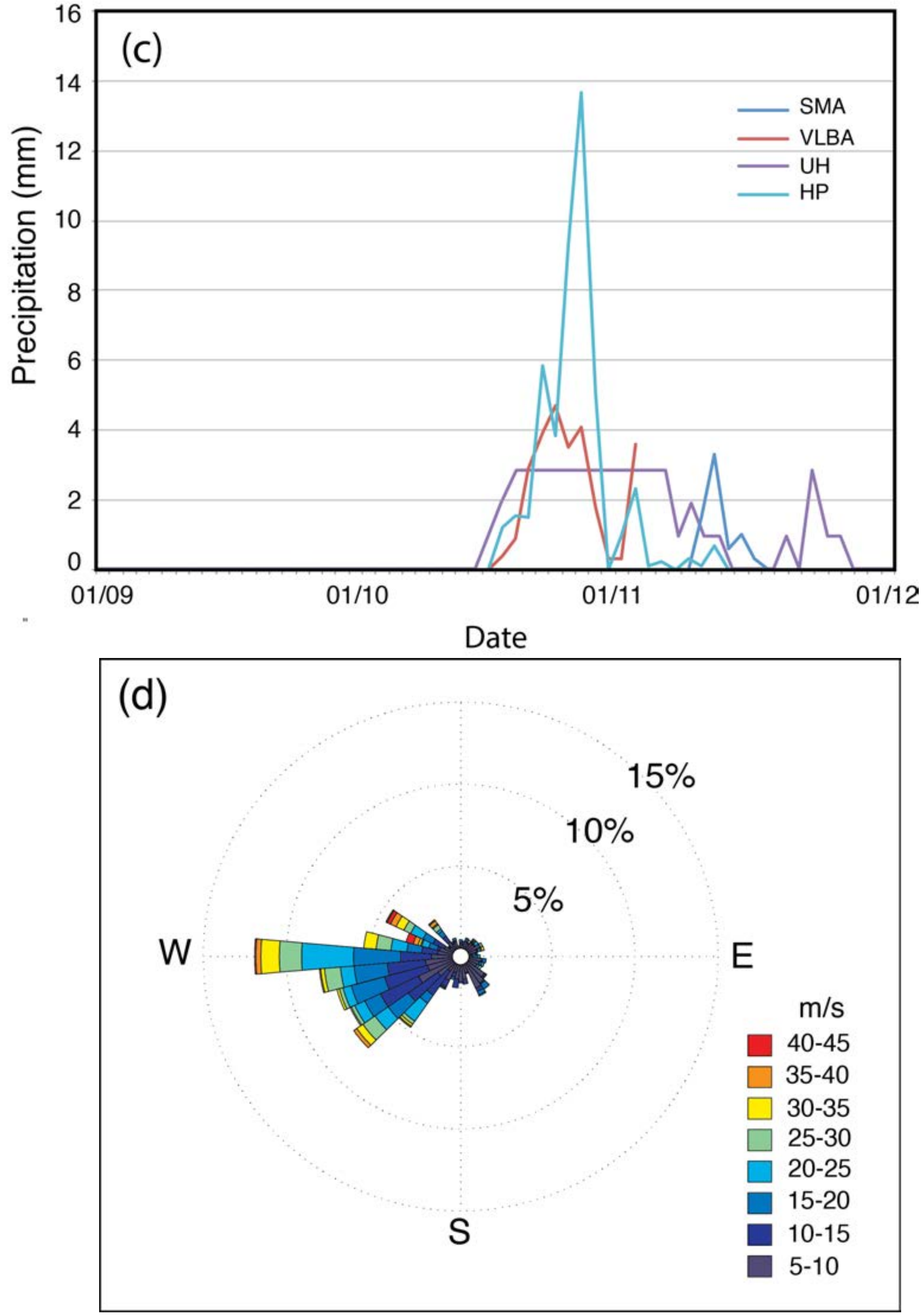

FIGURE 5. continued Mauna Kea summit c) Precipitation from 1200 UTC 09 January to 2300 UTC 11 JANUARY 2011. d) Wind rose plot of Mauna Kea summit wind speeds and directions from 1000 UTC 09 January to 0900 UTC 11 JANUARY 2011.

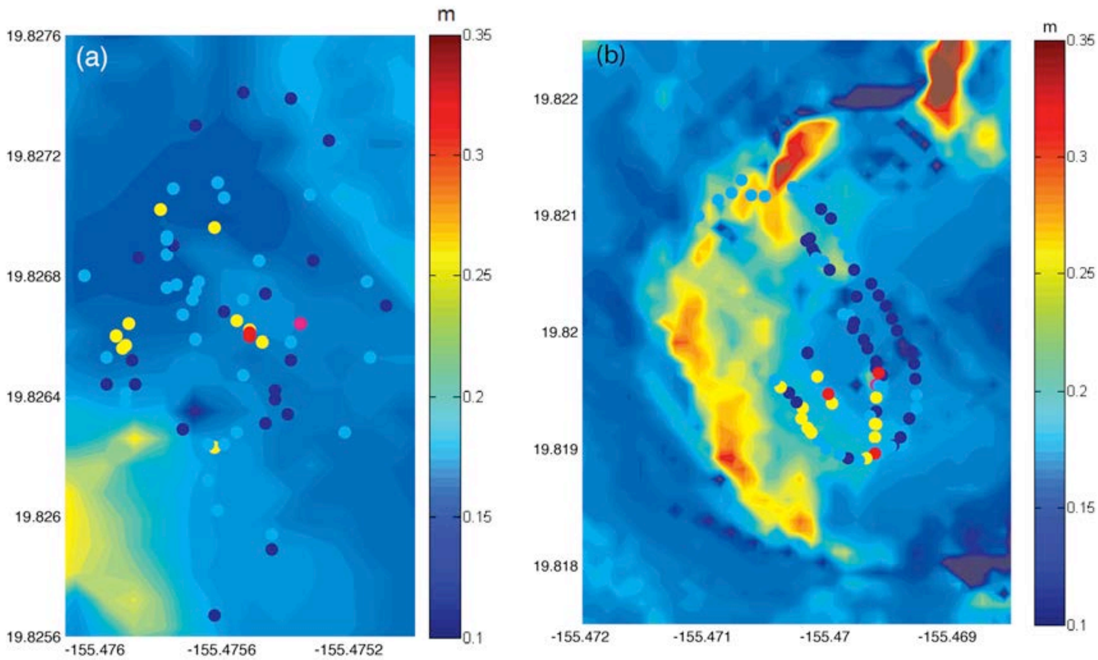

FIGURE 6. a) Pu‘u Hau‘oki and b) Pu‘u Wēkiu modeled snow depth (color contours) for 0959 UTC 11 January 2011; snow depth observations (colored dots) between 2130 UTC 11 January and 0000 UTC 12 January 2011.

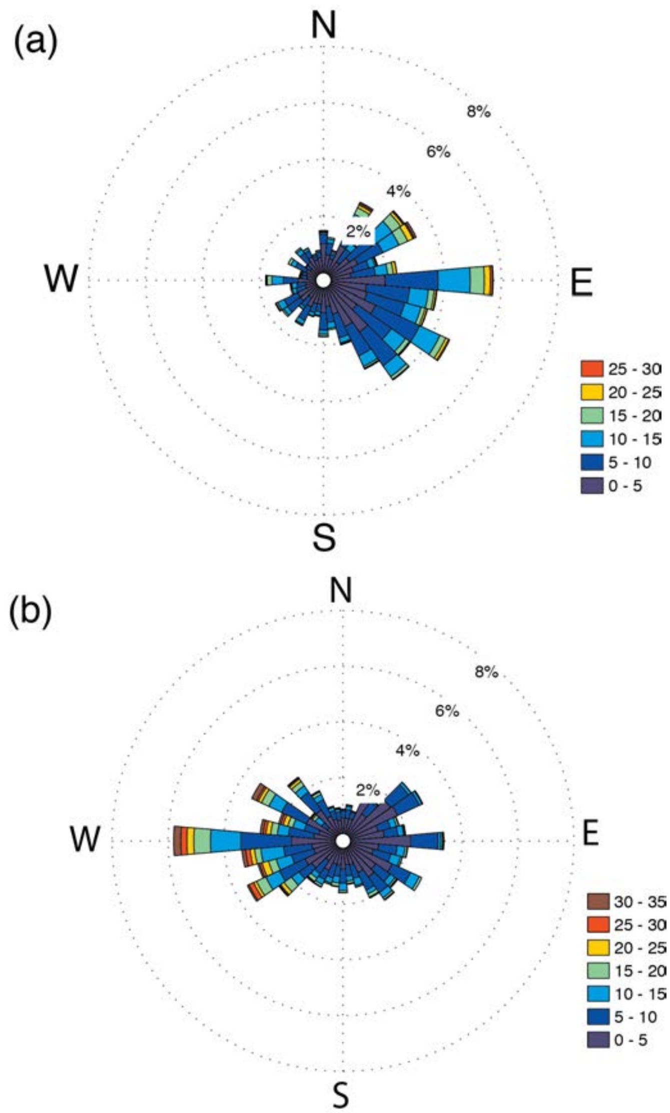

FIGURE 7. Wind rose of winds during snow events only for a) 2008 and b) 2009.

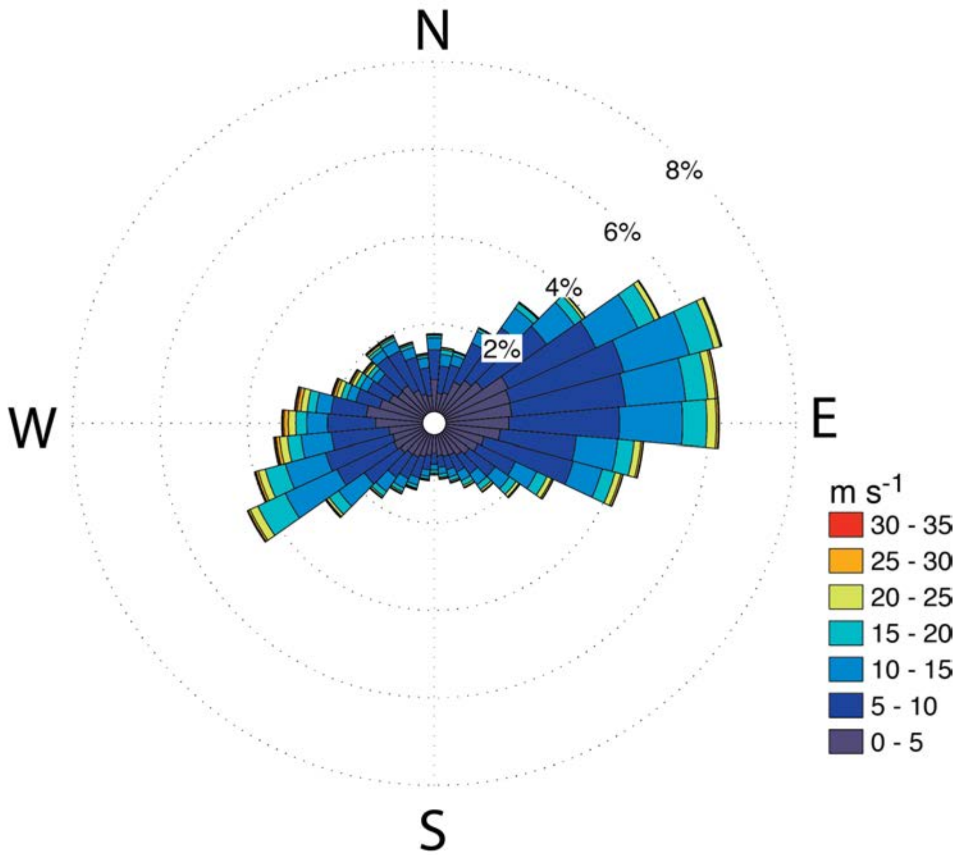

FIGURE 8. Wind rose for all Mauna Kea summit winds during for January 2008 through December 2010.

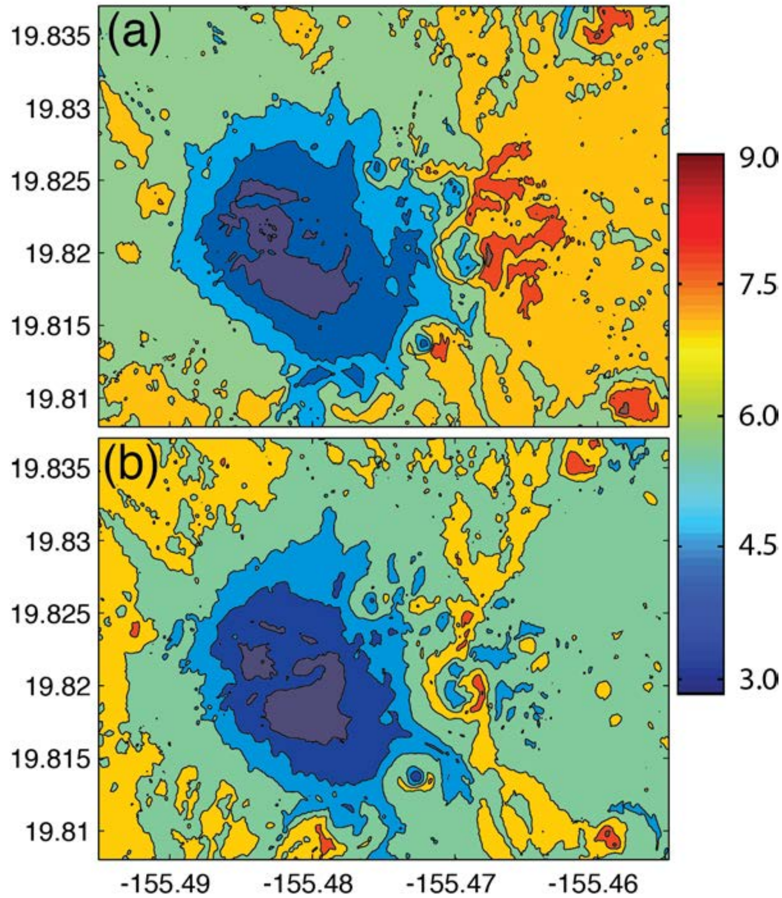

FIGURE 9. Modeled wind speed ($m\ s^{-1}$) from cardinal wind fields: a) east, b) west.

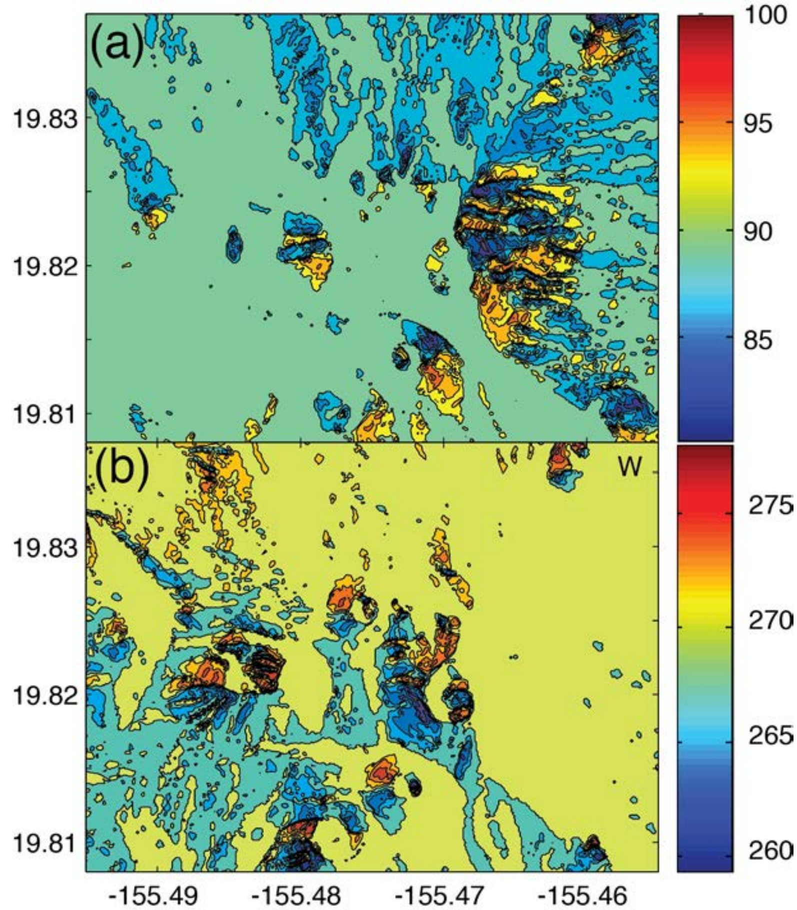

FIGURE 10. Modeled wind direction from cardinal wind fields: a) east, b) west.

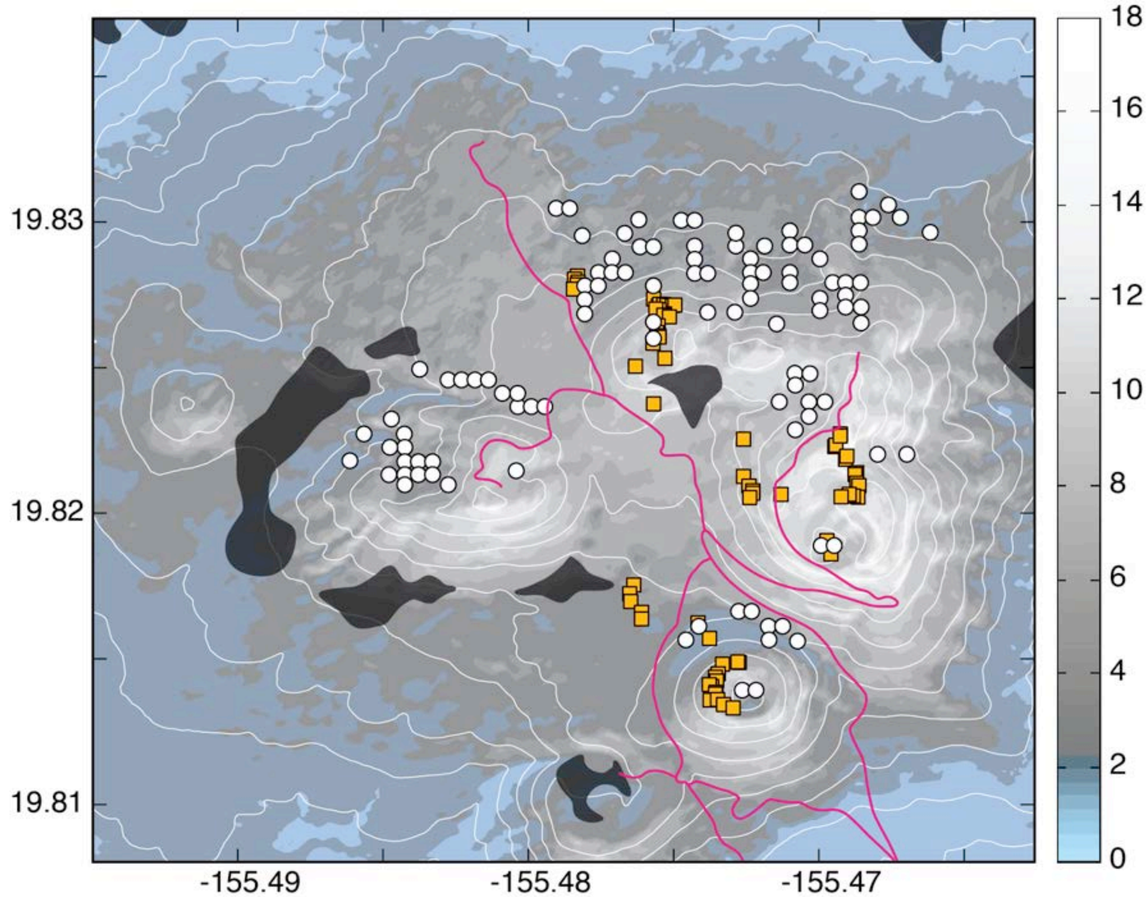

FIGURE 11. Modeled snow depth (in m, shading) and elevation (white contours) of Mauna Kea summit for the 2-year total from 2008-2009, and Wēkiu Bug trap locations from 2002-2008 with positive capture rates (yellow boxes), permafrost locations (white circles). Red lines indicate roads and dark shading indicates areas of lava flows and glacial till found to be unsuitable as wēkiu bug habitat.

H

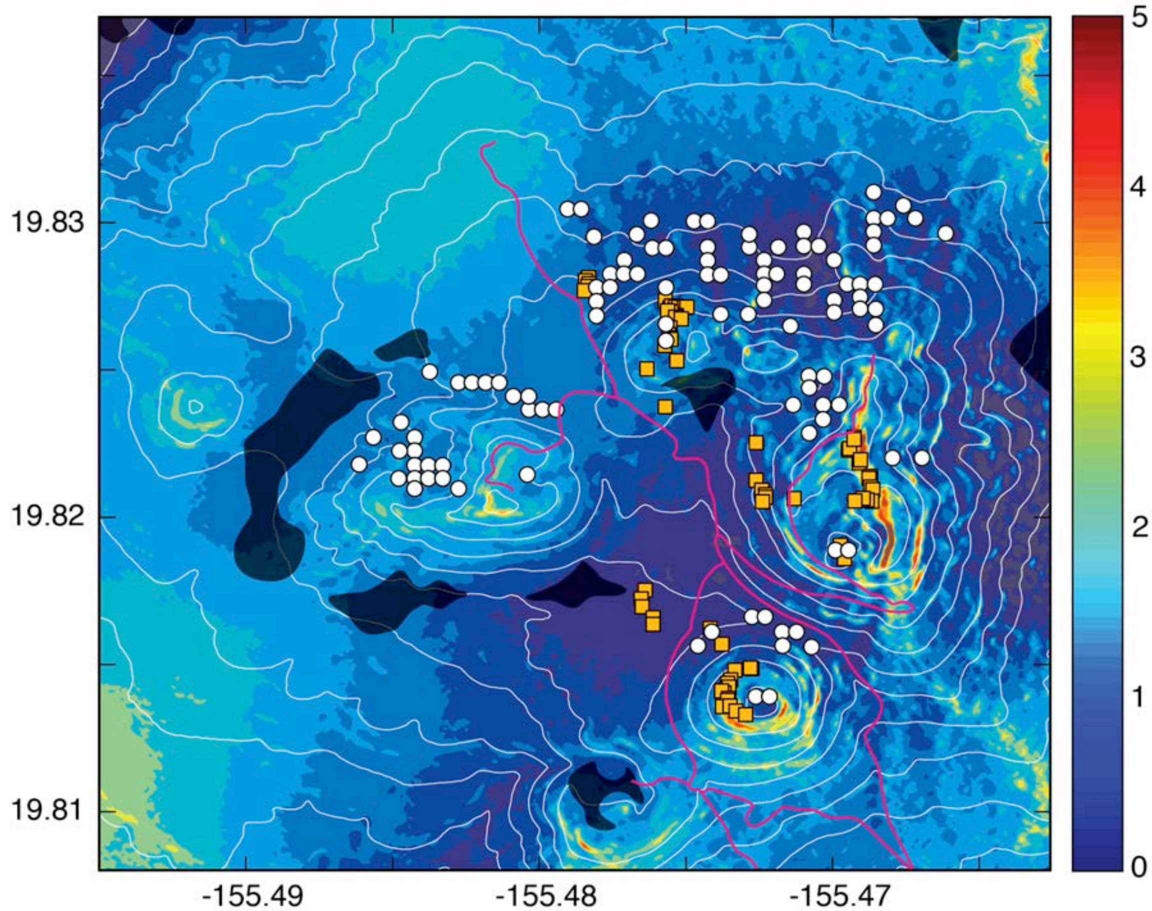

FIGURE 12. As in Fig. 11, but for modeled bug fall density (undefined relative scale, colored shading) on Mauna Kea for 3-year total from 2008 through 2010.

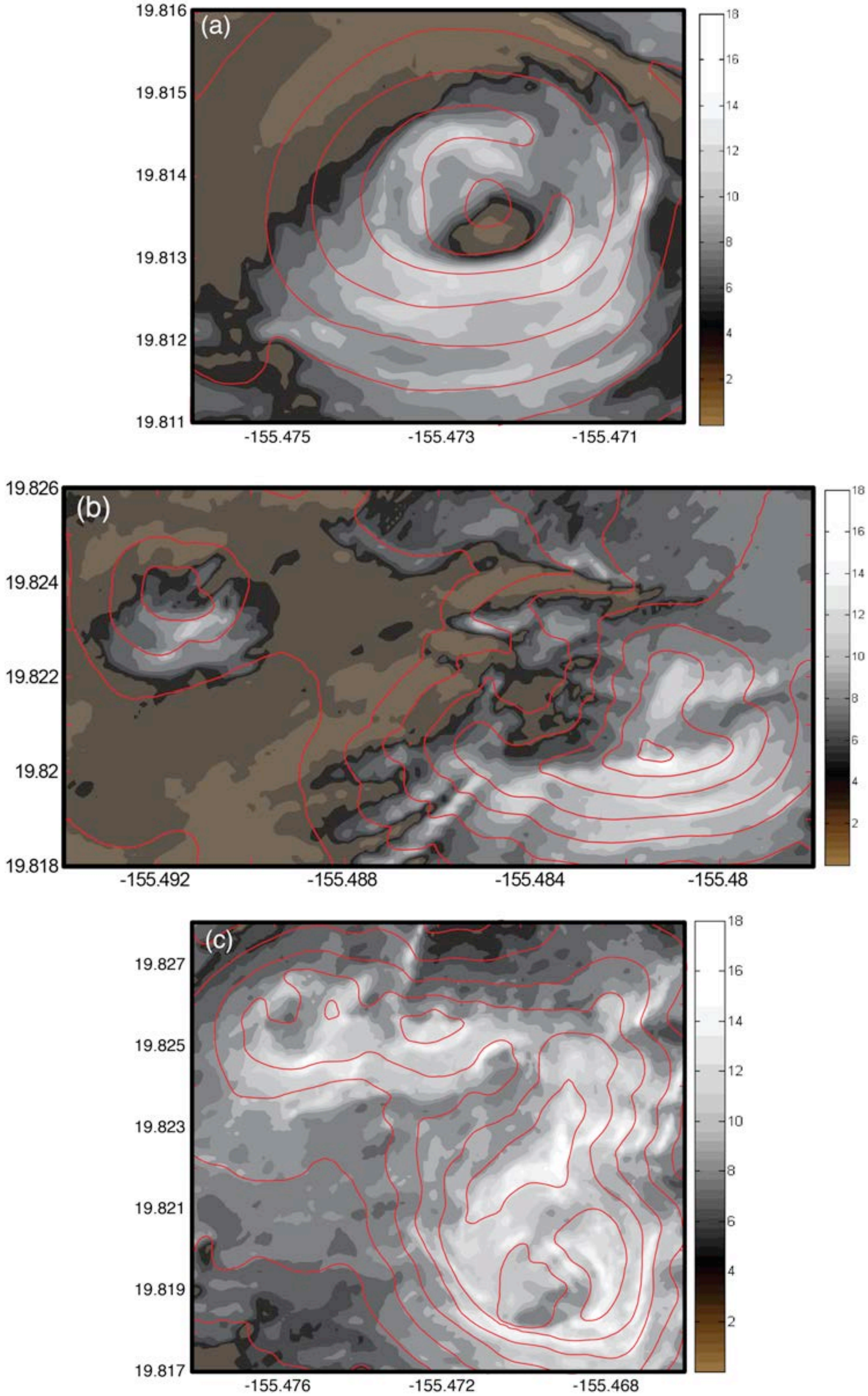

FIGURE 13. Same as Fig. 11 but with elevation contours in red, but for a) Pu‘u Haukea; b) Pu‘u Pōhaku and Pu‘u Poli‘ahu; and c) Pu‘u Hau‘oki and Pu‘u Wēkiu.

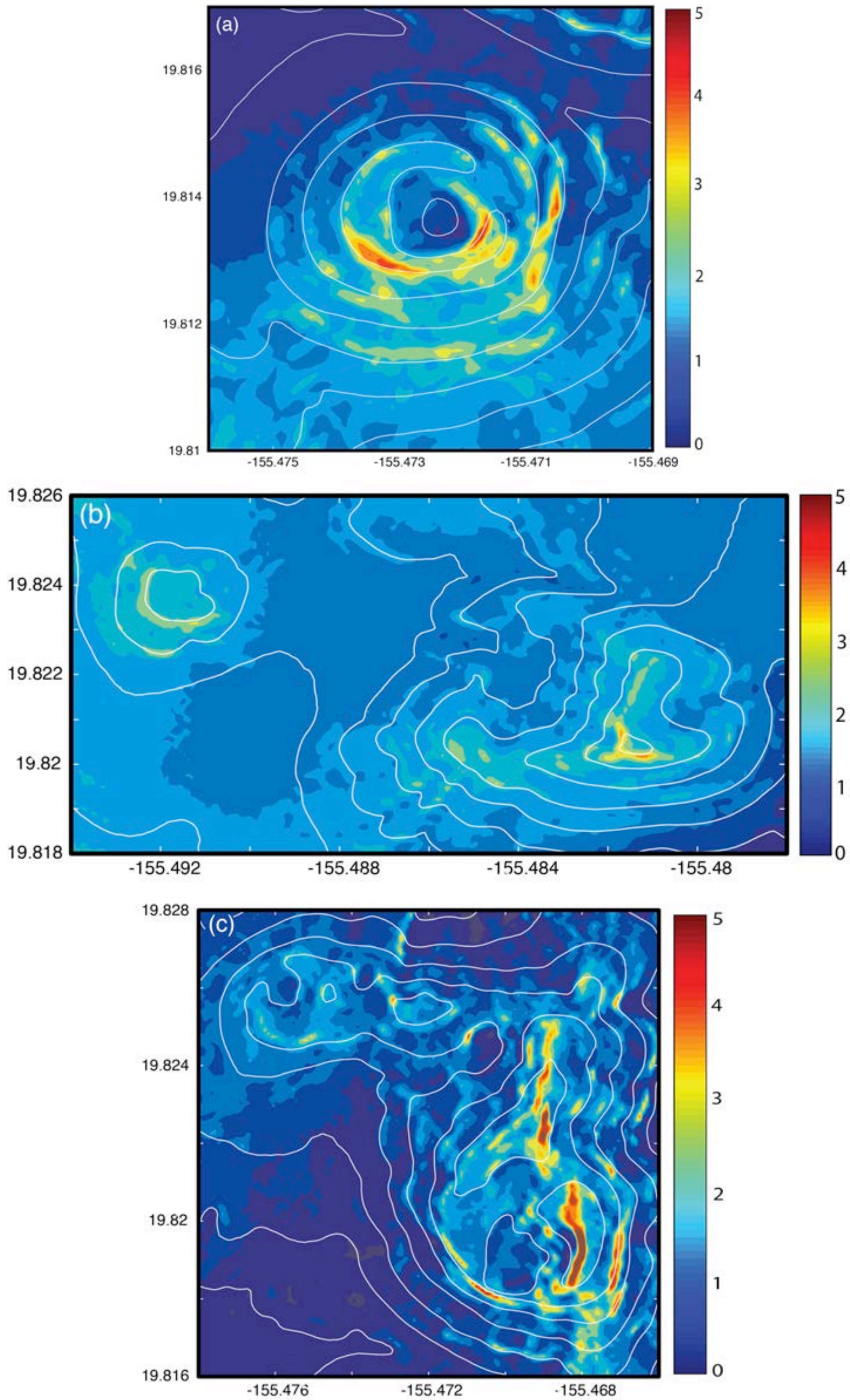

FIGURE 14. Same as Fig. 12 but for a) Pu‘u Haukea; b) Pu‘u Pōhaku and Pu‘u Poli‘ahu; and c) Pu‘u Hau‘oki and Pu‘u Wēkiu.